RAPID COMMUNICATIONS

PHYSICAL REVIEW B VOLUME 40, NUMBER 8 15 SEPTEMBER 1989-I

# Atomic-resolution scanning-tunneling-microscopy investigations of alkali-metal–graphite intercalation compounds

Stephen P. Kelty and Charles M. Lieber
*Department of Chemistry, Columbia University, New York, New York 10027*

(Received 5 June 1989)

The scanning tunneling microscope has been used to image stage-1 and stage-2 potassium, rubidium, and cesium graphite intercalation complexes with atomic resolution. Images of the stage-1 materials exhibit a 2**a** modulation for a wide range of tunneling currents (0.5–10 nA) and bias voltages (−750 to +750 mV). This new superlattice is also ordered over large ($> 500 \times 500$ Å$^2$) areas. Images of the stage-2 materials are dominated by a centered hexagonal structure typical of graphite. The vertical corrugation determined for the stage-2 materials is, however, significantly smaller than observed for graphite. These results are discussed with respect to theoretical explanations of the anomalous features observed in images of graphite.

Scanning-tunneling-microscopy (STM) images of the surface of highly oriented pyrolytic graphite (HOPG) often exhibit two anomalous features, including: (1) large ($\geq 1$ Å) vertical corrugations between the atomic positions and the centers of the carbon rings, and (2) a large asymmetry between adjacent carbon atom sites (usually only alternate atoms are observed).[1-8] Current evidence suggests that large vertical corrugations are due to elastic interactions mediated by a contamination layer between the tip and the graphite surface,[4] although other factors may also be important.[2,3,5] Asymmetry between adjacent carbon atoms in images of HOPG has been explained by the unique electronic properties (near the Fermi level, $E_F$) of the two structurally distinct carbon sites in graphite.[6-8] These site differences are intrinsic to hexagonal graphite which has an *AB* stacking sequence [Fig. 1(a)]. The graphite stacking sequence and electronic structure can, however, be modified by intercalation of electron donor and acceptor species.[9] Hence, it has been suggested that STM studies of graphite intercalation complexes (GIC's) should provide data useful for elucidating further the origins of these interesting anomalies.[2,8,10-13]

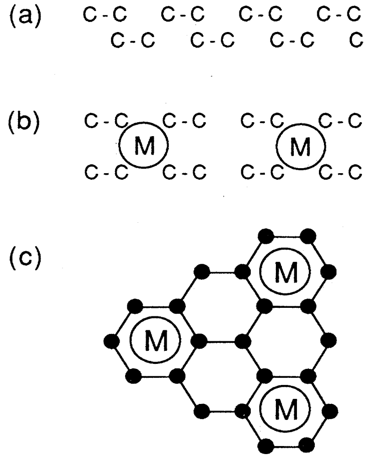

FIG. 1. Cross-sectional view of (a) hexagonal graphite and (b) a stage-1 GIC. (c) Top view of the stage-1 GIC illustrating the commensurate 2×2 structure.

In this Rapid Communication we report the first systematic atomic-resolution STM investigations of stage-1 and stage-2 potassium, rubidium, and cesium intercalation compounds. Recently, a STM investigation of the $\mathrm{LiC_6}$ GIC was reported.[12] Hexagonal structures with in-plane periods larger than HOPG were observed in $\mathrm{LiC_6}$ and attributed to images of lithium metal on the graphite surface. For the GIC's studied herein, however, it is believed that at room temperature all of the alkali metal is intercalated (i.e., there is no metal on the surface).[14,15] The carbon layer stacking in the stage-1 ($M\mathrm{C_8}$) K, Rb, and Cs GIC's is *AA* [Fig. 1(b)] and intercalation of the three metals increases the carbon layer-layer spacing by 2, 2.3, and 2.7 Å, respectively.[9] In addition, diffraction evidence suggests that the alkali-metal ions form an ordered 2**a**×2**a** lattice in the bulk[16] and at the surface[14,17] of these $M\mathrm{C_8}$ materials [Fig. 1(c)]. The carbon-intercalant-carbon stacking is also believed to be *AA* in the stage-2 GIC's (and *AB* between adjacent carbon layers),[16] although the alkali-metal layer is disordered at room temperature.[18-20] In our STM studies we find that images of the stage-1 Rb and Cs GIC's exhibit a strong 2**a** ($a = 2.46$ Å) modulation similar to our recent report for $\mathrm{KC_8}$.[13] This new superstructure has been observed for bias voltages up to $|750\ \mathrm{mV}|$ and for tunneling currents between 0.5 and 10 nA, and is ordered over large areas. Images of the stage-2 materials are dominated by a centered hexagonal structure typical of graphite. The vertical corrugation determined for the stage-2 materials is, however, significantly smaller than observed for HOPG.

The stage-1 and stage-2 GIC's were prepared from HOPG (Union Carbide) and alkali metal ($> 99.9\%$) using the standard two-zone technique.[9,16] The GIC samples were removed from the sealed reaction tubes inside an argon filled glovebox that was equipped with a purification system capable of reducing the oxygen and water concentration to $< 1$ ppm. The optical properties and elemental analysis results were consistent with bulk formulations of $M\mathrm{C_8}$ and $M\mathrm{C_{24}}$ for the stage-1 and stage-2 materials, respectively. The STM experiments were carried out in the glovebox (without exposing the samples to air) using a commercial STM (Ref. 21) and mechanically formed platinum-iridium alloy tips. The samples could be cleaved repeatedly after mounting on the STM stage to expose new surfaces that were stable for at least 4 h. Although alkali-metal may be left on the surface immediately after cleaving a sample, previous studies of K and Cs overlayers on graphite have shown that such surface metal will rapidly intercalate at 300 K.[14,15]

Typical constant current images of $RbC_8$ and $CsC_8$ are shown in Fig. 2. Lighter areas in these images correspond to apparent surface protrusions while darker areas indicate depressions. Under this bias condition tunneling occurs from sample to tip and thus images depict the filled sample states near $E_F$. The images of $RbC_8$ and $CsC_8$ are very similar to that observed for $KC_8$ (Ref. 13) and are different than images observed for graphite. In particular, the images of $RbC_8$ and $CsC_8$ exhibit a long-range modulation of period $4.9 \pm 0.5$ Å ($p$ sites) and two other inequivalent sites, $p'$ and $p''$ [Fig. 2(b)]; the $p$-$p'$, $p$-$p''$, and $p'$-$p''$ distances are all ca. 2.5 Å. Images such as Fig. 2(a) and 2(b) are reproducibly observed for tunneling currents between 0.5 and 10 nA (bias-voltage −15 mV) and for bias voltages between −750 and 750 mV. The vertical corrugation (at constant tip height) remains nearly constant over this bias-voltage range. Furthermore, pairs of images acquired simultaneously at positive and negative bias voltages have an identical registry of the $p$, $p'$, and $p''$ features. We also find that the **2a** superlattice is stable and ordered over areas at least as large as 500×500 Å$^2$ (Fig. 3). We therefore believe that these new features are not due to contamination, multiple-tip imaging, or isolated defects.[22-24]

Several explanations could account for the new **2a** modulation observed in our images of K, Rb, and Cs stage-1 GIC's. First, it is possible that the **2a** superlattice corresponds to a direct image of the metal sites. Direct imaging of Li on the surface of $LiC_6$ has been proposed to explain experimental results for this GIC.[12] For K, Rb, and Cs GIC's previous studies[14,15] have shown that there is no alkali-metal on the surface (this may also be true in the case of lithium[14]), although the intercalant layer beneath the graphite surface does have a **2a** periodicity.[17] It is unlikely, however, that the **2a** superlattice in our images corresponds directly to these sites since the lowest energy metal states (the empty *ns* level) lie several eV above the Fermi level. Furthermore, such an assignment would be inconsistent with the 2.5-Å lattice spacing observed for the $p'$ and $p''$ features since the alkali-metal ions are located at the centers of the carbon hexagons. It is also possible that the **2a** modulation is due to a variation in the force between the sample and tip[25] caused by the underlying 2×2 metal ion lattice. We believe that this is unlikely since images obtained in the constant height mode where the sample-tip force remains nearly constant[7] also exhibit the new **2a** superlattice. Hence, we suggest that the observed **2a** modulation has an electronic origin. In fact, detailed electronic structure calculations suggest that a new

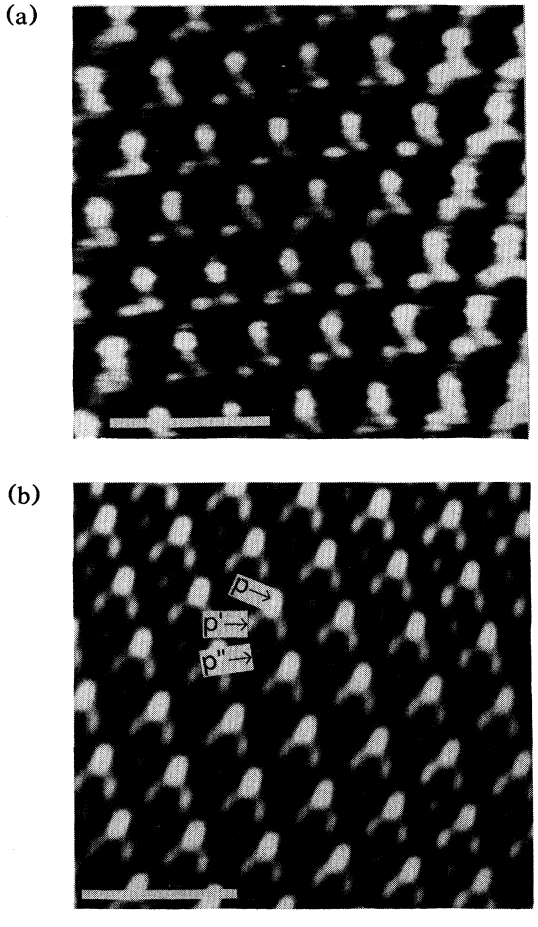

FIG. 2. (a) Constant current image of $CsC_8$ recorded with a sample vs tip bias voltage of −15 mV and 8-nA tunneling current. (b) Image of $RbC_8$ recorded with a −15-mV bias voltage and 4-nA tunneling current; the $p$, $p'$, and $p''$ sites are marked in one unit cell. The bar in both images corresponds to 10 Å.

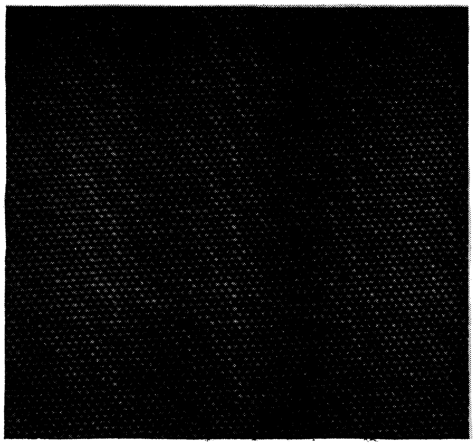

FIG. 3. 300×300 Å$^2$ constant current image of $CsC_8$ recorded with −15-mV bias voltage and a 6-nA tunneling current. The centered hexagonal structure has a period of 4.9 Å (**2a**) which is the same as the $p$-$p$ distance in Fig. 2. The $p'$ and $p''$ sites are not resolved in this image.

low-dispersion interlayer band should be present in the stage-1 $MC_8$ compounds near $E_F$.[26,27] The presence of a low-dispersion band near $E_F$ has been confirmed experimentally in angle-resolved photoelectron spectroscopy (ARPES) studies of $KC_8$ and $CsC_8$.[17,28] In addition, it has been proposed that this band is due to a surface driven charge density wave.[28] The 2**a** modulation observed in our STM images of the $MC_8$ GIC's may correspond to a real-space observation of such a charge modulation, although additional studies will clearly be needed to identify unambiguously the origin of this interesting feature.

To further probe these interesting results we have imaged the stage-2 materials. Figure 4 shows grey-scale images of the K and Rb GIC's recorded in the constant current mode. These images are typical of those obtained for several independently prepared stage-2 samples. Notably, the centered hexagonal structure and the 2.5 ± 0.2 Å lattice period determined from these images are similar to results obtained for HOPG.[1-8] The 0.4 ± 0.2 Å vertical corrugation is, however, lower than the 0.8 ± 0.3 Å value measured for graphite. This decrease in vertical corrugation is consistent with the expansion of the Fermi surface that occurs following alkali-metal intercalation.[2,10] The graphitelike features dominate experimental images recorded with bias voltages between −100 and 100 mV and tunneling currents between 2 and 20 nA. We do not observe new superlattice features in these stage-2 materials (in contrast to the 2**a** modulation in the $MC_8$ GIC's), although a low-amplitude ($\leq 0.05$ Å) modulation cannot be ruled out. To understand fully the origin of the observed differences between images of the stage-1 and stage-2 materials will require additional experimental and theoretical work. For example, it will be interesting to image the stage-2 materials at lower temperatures where the intercalant layers form ordered domains that are structurally similar to the room-temperature intercalant layers in the stage-1 GIC's.[18-20]

Finally, we compare these results for the stage-1 and stage-2 materials with theoretical investigations of graphite STM images. Calculations[6-8,10] have shown that all of the surface carbon atoms should be imaged equally in the stage-1 materials using a single-atom tip since intercalation removes the carbon-site asymmetry present in HOPG.[29] Although our experimental images for the $MC_8$ compounds exhibit a more complicated structure, these results are consistent with the low-dispersion band that has been observed in ARPES studies.[17,28] For the stage-2 materials recent tight-binding calculations also indicate that all of the surface carbon sites should be observed due to the expansion of the Fermi surface.[10] In contrast to the predictions of these calculations, our images for the stage-2 K, Rb, and Cs GIC's exhibit the centered hexagonal structure typical of native HOPG. The reduced vertical corrugation in these images is, however, consistent with an expanded Fermi surface. One possible explanation for these experimental observations is that the near surface region consists of two carbon layers with *AB* stacking as in HOPG,[30] although other factors may also be important.[5] Detailed theoretical calculations for this structural geometry should elucidate this point further.

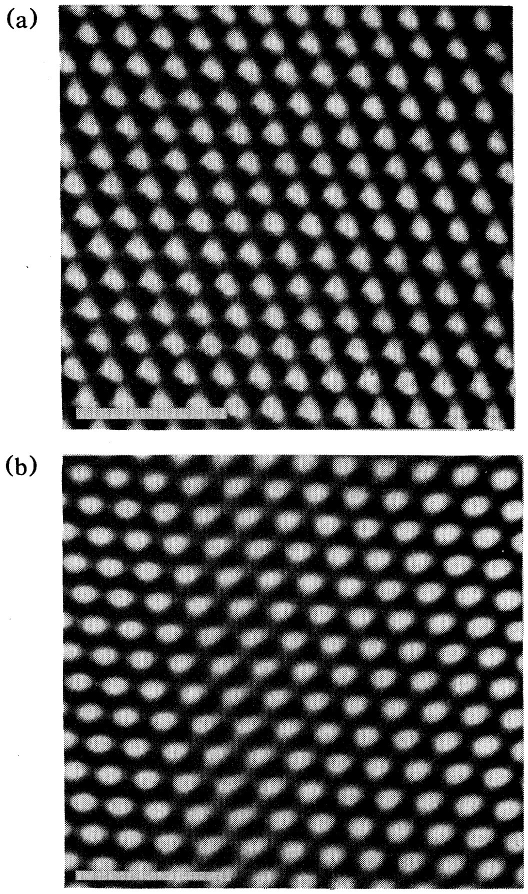

FIG. 4. (a) Unfiltered grey-scale image of $KC_{24}$ recorded with a −15-mV bias voltage and a 10-nA tunneling current. (b) Filtered image of the stage-2 rubidium GIC recorded with a −15-mV bias voltage and 6-nA tunneling current. Both images exhibit centered hexagonal structure with a period of 2.5 Å. The bar in both images corresponds to 10 Å.

In conclusion, we have used the STM to investigate the stage-1 and stage-2 alkali-metal GIC's with atomic resolution. We find that images of the stage-1 complexes exhibit a new 2**a** modulation of the graphite structure that has an electronic origin. Images of the stage-2 compounds exhibit the centered hexagonal structure typical of HOPG, although the vertical corrugation is significantly smaller than observed for graphite. These experimental results can be attributed in part to an expansion of the Fermi surface following intercalation, although additional electronic structure calculations will be needed to fully understand these interesting results.

We thank Dr. A. W. Moore (Union Carbide) for the donation of HOPG samples. C.M.L. acknowledges support of this work by The David and Lucile Packard Foundation, the National Science Foundation (CHE-8857-194), and Rohm and Haas Company.

---

[1] G. Binnig, H. Fuchs, Ch. Gerber, H. Rohrer, E. Stoll, and E. Tosatti, Europhys. Lett. **1**, 31 (1986).

[2] J. Tersoff, Phys. Rev. Lett. **57**, 440 (1986).

[3] J. M. Soler, A. M. Baro, N. Garcia, and H. Rohrer, Phys. Rev. Lett. **57**, 444 (1986).

[4] H. J. Mamin, E. Ganz, D. W. Abraham, R. E. Thomson, and J. Clarke, Phys. Rev. B **34**, 9015 (1986).

[5] J. B. Pethica, Phys. Rev. Lett. **57**, 3235 (1986).

[6] I. P. Batra, N. Garcia, H. Rohrer, H. Salemink, E. Stoll, and S. Ciraci, **181**, 126 (1987).

[7] D. Tomanek, S. G. Louie, H. J. Mamin, D. W. Abraham, R. E. Thomson, E. Ganz, and J. Clarke, Phys. Rev. B **35**, 7790 (1987).

[8] D. Tomanek and S. G. Louie, Phys. Rev. B **37**, 8327 (1988).

[9] M. S. Dresselhaus and G. Dresselhaus, Adv. Phys. **30**, 139 (1981).

[10] X. Qin and G. Kirczenow, Phys. Rev. B **39**, 6245 (1989).

[11] S. Gauthier, S. Rousset, J. Klein, W. Sacks, and M. Belin, J. Vac. Sci. Technol. A **6**, 360 (1988).

[12] D. Anselmetti, R. Wiesendanger, and H. J. Guntherodt, Phys. Rev. B **39**, 11 135 (1989).

[13] S. P. Kelty and C. M. Lieber, J. Phys. Chem. **93**, 5983 (1989).

[14] M. T. Johnson, H. I. Starnberg, and H. P. Hughes, Surf. Sci. **178**, 290 (1986).

[15] M. T. Johnson, H. I. Starnberg, and H. P. Hughes, Solid State Commun. **57**, 545 (1986).

[16] D. E. Nixon and G. S. Parry, J. Phys. D **1**, 291 (1968).

[17] N. Gunasekara, T. Takahashi, F. Maeda, T. Sagawa, and H. Suematsu, J. Phys. Soc. Jpn. **56**, 2581 (1987).

[18] A. N. Berker, N. Kambe, G. Dresselhaus, and M. S. Dresselhaus, Phys. Rev. Lett. **45**, 1452 (1980).

[19] D. M. Hwang, N. W. Parker, M. Utlaut, and A. V. Crewe, Phys. Rev. B **27**, 1458 (1983).

[20] F. Rousseaux, R. Moret, D. Guerard, P. Lagrange, and M. Lelaura, Synth. Met. **12**, 45 (1985).

[21] Nanoscope, Digital Instruments, Inc., Santa Barbara, CA.

[22] H. A. Mizes and J. S. Foster, Science **244**, 559 (1989).

[23] T. R. Albrecht, H. A. Mizes, J. Nogami, S. I. Park, and C. F. Quate, Appl. Phys. Lett. **52**, 362 (1988).

[24] If these new features were due to multiple tip or contamination effects they would only be observed intermittently.

[25] C. M. Mate, R. Erlandsson, G. M. McClelland, and S. Chiang, Surf. Sci. **208**, 473 (1989).

[26] H. Kamimura, Ann. Phys. (Paris) **11**, Suppl. 2, 39 (1986).

[27] R. C. Tatar and S. Rabii, in *Graphite Intercalation Compounds,* edited by P. Eklund, M. S. Dresselhaus, and G. Dresselhaus (Materials Research Society, Pittsburgh, 1984), p. 71.

[28] D. Marchand, C. Fretigny, N. Lecomte, and M. Lagues, Synth. Met. **23**, 165 (1988).

[29] For low-resolution imaging conditions the surface would appear featureless.

[30] Cleavage of the stage-2 samples between carbon-intercalant-carbon layers would leave a carbon layer at the surface and directly below the surface.

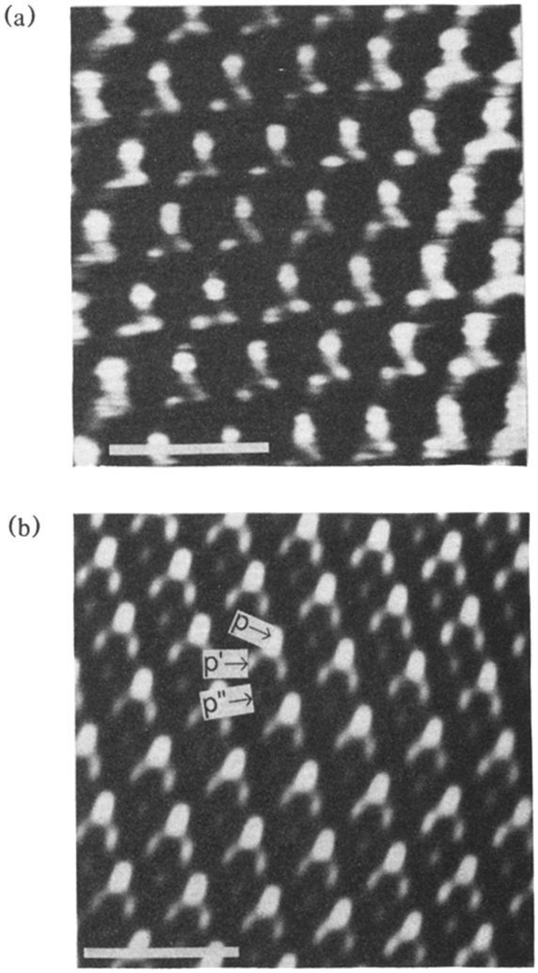

FIG. 2. (a) Constant current image of $CsC_8$ recorded with a sample vs tip bias voltage of $-15$ mV and 8-nA tunneling current. (b) Image of $RbC_8$ recorded with a $-15$-mV bias voltage and 4-nA tunneling current; the $p$, $p'$, and $p''$ sites are marked in one unit cell. The bar in both images corresponds to 10 Å.

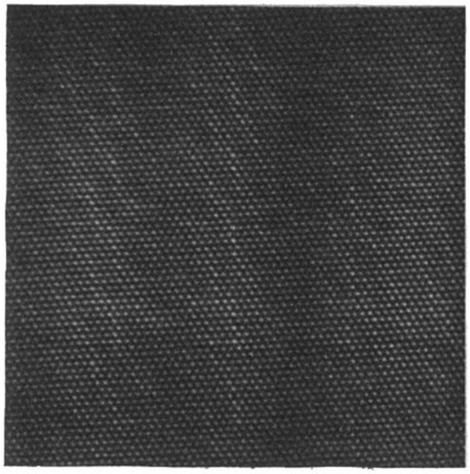

FIG. 3. 300×300 Å$^2$ constant current image of $CsC_8$ recorded with −15-mV bias voltage and a 6-nA tunneling current. The centered hexagonal structure has a period of 4.9 Å (2**a**) which is the same as the *p*-*p* distance in Fig. 2. The $p'$ and $p''$ sites are not resolved in this image.

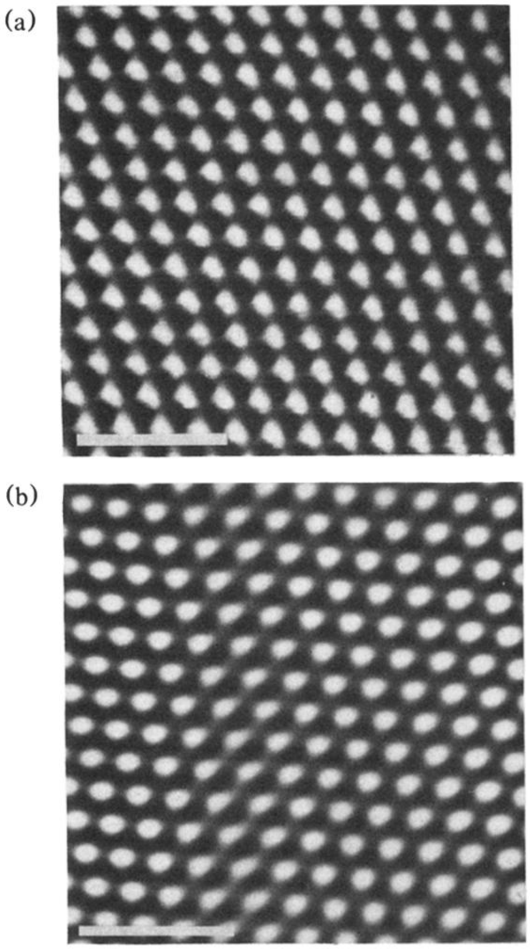

FIG. 4. (a) Unfiltered grey-scale image of $KC_{24}$ recorded with a −15-mV bias voltage and a 10-nA tunneling current. (b) Filtered image of the stage-2 rubidium GIC recorded with a −15-mV bias voltage and 6-nA tunneling current. Both images exhibit centered hexagonal structure with a period of 2.5 Å. The bar in both images corresponds to 10 Å.